HHS Public Access

Author manuscript

ACS Sens. Author manuscript; available in PMC 2019 March 23.

Published in final edited form as:

ACS Sens. 2018 March 23; 3(3): 640–647. doi:10.1021/acssensors.7b00912.

Implications of Thermal Annealing on the Benzene Vapor Sensing Behavior of PEVA-Graphene Nanocomposite Threads

Sanjay V. Patel[†,*], **Sabina Cemalovic**[†], **William K. Tolley**[†], **Stephen T. Hobson**[†,§], **Ryan Anderson**[‡], and **Bernd Fruhberger**[‡]

[†]Seacoast Science, Inc., 2151 Las Palmas Drive, Suite C, Carlsbad, California 92011, United States

[‡]University of California, San Diego9500 Gilman Drive, La Jolla, California. 92093, United States

Abstract

The effect of thermal treatments, on the benzene vapor sensitivity of polyethylene (co-)vinylacetate (PEVA)/graphene nanocomposite threads, used as chemiresistive sensors, was investigated using DC resistance measurements, differential scanning calorimetry (DSC), and scanning electron microscopy (SEM). These flexible threads are being developed as low-cost, easy-to-measure chemical sensors that could be incorporated into smart clothing or disposable sensing patches. Chemiresistive threads were solution-cast or extruded from PEVA and <10% graphene nanoplatelets (by mass) in toluene. Threads were annealed at various temperatures and showed up to 2 orders of magnitude decrease in resistance with successive anneals. Threads heated to ≥80 °C showed improved limits of detection, resulting from improved signal–noise, when exposed to benzene vapor in dry air. In addition, annealing increased the speed of response and recovery upon exposure to and removal of benzene vapor. DSC results showed that the presence of graphene raises the freezing point, and may allow greater crystallinity, in the nanocomposite after annealing. SEM images confirm increased surface roughness/area, which may account for the increase response speed after annealing. Benzene vapor detection at 5 ppm is demonstrated with limits of detection estimated to be as low as 1.5 ppm, reflecting an order of magnitude improvement over unannealed threads.

Graphical Abstract

[*]Corresponding Author: sanjay@seacoastscience.com.

[§]**Present Address**

Department of Biology & Chemistry, Liberty University, 1971 University Blvd, Lynchburg, VA 24515

ORCID

Sanjay V. Patel: 0000-0001-9540-9957

Author Contributions

The manuscript was written through contributions of all authors.

Notes

The authors declare no competing financial interest.

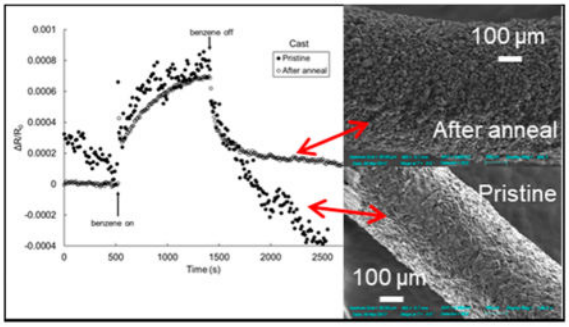

Keywords

graphene; polymer nanocomposite; PEVA; chemical sensor; benzene vapor sensor; exposure monitor; chemiresistor; wearable sensors

Poly(ethylene-*co*-vinylacetate) (PEVA) is a semicrystalline polymer at room temperature, and has been studied extensively for use in vapor sensors,[1–3] wire insulation,[4] shrinkable and moldable parts,[5,6] and thermal conduction materials.[7] PEVA is a copolymer, with a reported glass transition temperature (T_g) near −30 °C[8] and a melting temperature (T_m) in the range of 85–88 °C.[4,9–11] Polymer–nanocomposite chemiresistors (PNCs) in general, and PEVA-based chemiresistors in particular,[12–14] have been used for detecting a wide variety of airborne hazards. These PNCs typically contain an absorbing, insulating polymer to interact with analyte vapors and conductive dopant. The polymer swells during sorption of chemical vapors from the air, which causes an increase in resistance of the chemiresistor.[12,15] The conductive dopant in the PNCs have included gold nano-particles,[16] carbon nanotubes,[17] and graphene.[18,19] PEVA's low polarity[20] and poor hydrogen bonding character,[21] as indicated by Hansen solubility parameters ($\delta_{dispersion}$ = 19 MPa$^{1/2}$, δ_{polar} = 2 MPa$^{1/2}$, $\delta_{H\text{-}bonding}$ ~ 1 MPa$^{1/2}$), make it interesting for detecting low-polarity vapors, such as the hydrocarbons found in fuels. PEVA has been demonstrated to have a high affinity for benzene and other nonpolar chemicals when used in chemiresistors[12,13,15,19] and other sensor platforms.[22]

We previously demonstrated[19] the use of graphene in selective chemiresistors, and showed that an order-of-magnitude less graphene (by mass) could be used to create chemiresistors with similar conductivity, sensitivity, and performance to chemiresistors made with graphitic carbon black or carbon nanotubes. The selectivity and sensitivity of these devices were influenced by the type of polymer and the amount of conductive dopant.

In this work, we explore thermal treatments to PEVA-graphene nanocomposite threads to increase response speed and sensitivity toward benzene vapor. Resultant sensing threads are intended for use in "smart" clothing or disposable patches[19] with chemical sensing functionality.

EXPERIMENTAL SECTION

Materials

Pristine graphene (GR) powder was purchased from Angstron Materials (#N002-PDR, <3 graphene layers, x–$y \leq 10$ μm, Dayton, OH, www.angstronmaterials.com). Benzene, toluene, and poly(ethylene-*co*-vinylacetate) (PEVA-18% vinylacetate, #18,106–4) were purchased from Sigma-Aldrich Corporation (St. Louis, MO), and used as received.

Polymer–Graphene Suspensions

Sensor materials were fabricated as “threads”, using solution casting and solution extrusion. Before fabrication as threads, the polymer was dissolved in toluene, followed by addition of dry graphene nanoplatelet powder until the final desired concentration of solids was achieved. These suspensions were then sonicated for 1–3 h prior to use.

Solution Casting

Casting slurries were 5 wt % solids, which flow freely into a glass Petri dish. These slurries were allowed to air-dry at room temperature. Segments were then cut using a razor blade to obtain final chemiresistors, which were attached to forked pin rails using silver paste. The pin-rails allowed for secure physical and electrical connections during the vapor tests.

Solution Extrusion

Solution-extruded threads were formed by forcing the polymer–graphene suspensions through a standard glass 10 mL syringe and stainless steel needle cut to ~1/4 in. length to reduce the dead volume. Suspensions were typically >15 wt % solids (PEVA and graphene) to achieve sufficient viscosity for the extruded threads to retain their shape. These suspensions were used as the stock material; greater densities were obtained by allowing a portion of the solvent to evaporate from these stock solutions. Standard 18- and 22-gauge stainless steel needles were used as nozzles for extrusion of the chemiresistor threads. The threads were extruded at room temperature onto a microscope slide for support and allowed to dry prior to cementing segments of the threads to the forked pins for testing. After drying, the 18- and 22-gauge thread diameters were 0.46 mm ± 0.02 mm and 0.32 mm ± 0.03 mm, respectively. Finer gauge needles produced threads that were too fragile to handle.

Annealing and Testing

Threads were tested in a temperature-and humidity-controlled test system.[23,24] Benzene vapor was delivered by from a certified gas cylinder (100 ppm benzene in air, Matheson Tri-Gas, Inc., San Marcos, CA). Dried laboratory air from an air compressor was passed through Drierite as the carrier gas for all tests. Mass-flow controllers regulated dilution with dry or humidified air to produce the desired analyte concentrations. Chemical exposures were 15 min followed by a 45 min purge with analyte-free air. The baseline resistance (R_0) or resistance change, ΔR ($= R - R_0$), measured as the average of the 60 s before each change in environment, respectively. A computer-controlled multimeter (Agilent #34970A) was used to record the electrical resistance (2-point DC) of the sensors during testing. For this work, the noise is defined as the standard deviation of the baseline resistance over a 2 min period

(>10 data points) at 25 °C in dry air. Thermal anneals up to 70 °C in dry air were done in the same test system as the benzene vapor tests. Cooling rates were limited to ~0.7 °C/min due to the mass of the test system. For all anneals, the samples were first held at 25 °C for 6 h, then 6 h at the anneal temperature, and returned to 25 °C for 6 h. Annealing at >70 °C was done in the ambient lab air, without humidity control, in a Test Equity (105A) environmental chamber, capable of reaching 130 °C.

Differential Scanning Calorimetry (DSC)

Samples of solution-cast threads and pristine PEVA were submitted to Micromeritics Analytical Services (Norcross, GA) for DSC analyses (TA Instruments DSC, heated in air from −60 to 200 °C, at 10 °C/min, held 5 min, and cooled 200 to −60 °C at 10 °C/min).

Scanning Electron Microscopy (SEM)

SEM was performed at the NANO3 facility at UCSD. Pristine and 90 °C annealed samples of the solution-cast and solution-extruded materials were imaged in high vacuum mode with no metal coating using a Zeiss Sigma 500 SEM with an accelerating voltage of 0.8 kV.

RESULTS AND DISCUSSION

Influence of Annealing on Resistance and Benzene Response

Cast segments had lower starting resistance values, with bulk resistivity values (~0.2 Ω-m) compared against extruded threads (~1.3 Ω-m). Narrower gauge extrusions had higher DC electrical resistances (25 °C in dry air) than larger-diameter extrusions. In addition, cast segments were somewhat thicker (~0.9–1 mm), more rigid, and less fragile than the solution-extruded threads.

Several PEVA-GR 18- and 22-gauge extrusions were annealed in 10 °C increments, starting at 40 °C, and tested against benzene in dry air between anneals. Figure 1 shows the resistance of an extruded thread (22-gauge) recorded during the anneals.

During initial heating, from 25 °C to T_{anneal}, the resistance is seen to increase, briefly, then decreased in all cases. This is attributed to molecular rearrangement and thermal stress relief.[25,26] The resistance of all threads decreased, while at elevated temperature, with largest resistance shifts occurring at T_{anneal} = 50, 60, 70, and 80 °C. The resistance-change during the 90 °C treatment (after already being treated at 80 °C) is much smaller than the change occurring at any lower temperature.

Overall, from the initial pristine state to the post-90 °C annealed state, the baseline resistance (R_0 in 25 °C, dry air) dropped by a factor X ($X = R_{pristine}/R_{post\text{-}90\ °C}$), equal to 35 ± 22 and 90 ± 12, for the 18-gauge (n = 5) and 22-gauge (n = 4) solution-extruded threads, respectively. Note that the thinner, 22-gauge thread has the larger relative change from the heat treatment. The error stems from multiple sources. These segments were taken from multiple extrusions; therefore, uniformity from “first-out” extrusions to “last-out”, batch-to-batch variation, and thickness variations all are likely sources of poor thread-to-thread consistency. Finally, the silver-paste attachment may have added inconsistencies as the threads were annealed.

The direction of resistance-change upon cool-down from T_{anneal} to 25 °C reverses from a positive to a negative relation after the 80 °C treatment for all of the threads (Figure 1). During the first heating of the 18- and 22-gauge extruded threads, from 25 to 40 °C, the average temperature coefficient of resistance (TCR) was 0.00368 Ω/ Ω/°C ± 0.00060 Ω/ Ω/ °C, although the data are not linear in this regime. After the 90 °C anneal, the average TCR (measured from 20 to 40 °C) turned negative, and was −0.00057Ω/ Ω/°C ± 0.00004 Ω/ Ω/ °C for the extruded threads. The temperature sensitivity is reduced in addition to the change in behavior.

Figure 2 shows the benzene vapor response characteristics for two threads as pristine devices and after each of the incremental thermal treatments in Figure 1.

After each successive treatment, the responses ($\Delta R/R_0$) decreased until the 80 °C treatment for the solution-extruded threads.

Another effect of annealing was the reduction of noise in the baseline resistance (R_0), as measured with the same instrument. The ratio of noise to R_0 was reduced in threads, ranging from a factor of 2× to as much as 27×.

The limits of detection (LOD) were estimated from the raw data, using the IUPAC simplified relation (LOD = 3.29 × σ_0 × $C/\Delta R$), where σ_0 is the standard deviation of the baseline resistance, C is the concentration, and ΔR is the response amplitude due to chemical exposure.[27–29] The response magnitude decreased with successive anneals (Figure 2); however, the measured noise, with respect to the resistance baseline and vapor response, decreased proportionately more following annealing. This suggests improved dispersion of the graphene in the bulk.[30] Thus, the limits of detection (LOD), improved as the threads were annealed, with the most notable improvement occurring after the 70 °C anneal (Figure 3). Both the LOD and the exposure-to-exposure consistency (error bars are 1 SD) improved after the anneals.

These observations are consistent when new, pristine samples were heated directly to 60 °C, retested, and then heated to 90 °C and retested. When pristine samples were heated directly to 90 °C, the results are similar. Thus, the highest thermal treatment set the performance thereafter.

For comparison, solution-cast segments of longer slices were evaluated in parallel to the solution-extruded threads, and we observe that the behavior of these (thicker and denser) films is consistent with the extruded threads, with the exception that the starting and ending resistances are lower for the cast threads. After the 90 °C treatment, bulk resistivity of the cast threads was approximately 0.005 Ω-m, compared to 0.02 Ω-m for the extruded threads, which represent reduction by factors of 40 and 65 times, respectively. Reduced resistance is observed in some other polymer composites when heated above their T_m and is attributed to thermal stress relief.[25,26] We believe that, while the initial dispersion of graphene was different due to the two processing methods, the heat treatment has reduced the discrepancy after cooling.

Both types of samples were exposed to benzene vapors after each thermal treatment to compare sensitivity. Figure 4a,c shows the raw responses from pristine (left axes) and 90 °C-annealed samples (right axes).

The standard error (SE = standard deviation/average) of the baseline is 5.4×10^{-5} (pre anneal), and 6.7×10^{-6} post anneal. For ceramic 50 kOhm and 5 kOhm (1%) resistors in the same measurement setup, the SE was 6×10^{-6} and 2×10^{-6}, respectively. This suggests that the threads used as chemiresistors are more noisy in the preannealed state, rather than the noise being a measurement artifact.

After the 90 °C treatment, the baseline resistances are significantly lower, and the magnitude of the resistance change upon vapor exposure is also reduced. We also note that the resistance drift is reduced, and the speed of response to benzene vapor is increased after annealing, which is most obvious as the benzene vapor is removed from the system and the sensors recover to baseline. Figure 5 shows the time for the resistance of each type of thread (from Figure 4), to achieve 70%, of maximum response from baseline, and to recover 70% of the response back to baseline, before and after the 90 °C anneal.

After the 90 °C treatment, both response and recovery are faster on both types of threads, except at the lowest concentration in this test. We believe that this is likely due to slow concentration buildup of the vapor (from a bubbler with low flow), and due to the small responses of the unannealed threads; only 3–5 times the limit of detection. The large error bars (= ±1 SD) are attributed to the relatively large noise with the unannealed samples.

The inner diameter of an 18-gauge needle is 0.84 mm. During drying, as the toluene solvent evaporated from the solution-extruded threads, their average diameter reduced to 0.46 mm, indicating a significant reduction in bulk material volume. We note that annealing at the higher temperatures makes the threads more fragile. Additionally, annealing significantly alters the physical dimensions causing visible volume expansion, and, in extreme cases (Figure 6), resulted in cracking or breakage if both ends were held rigidly.

Table 1 lists the increase in thickness and length of both solution-cast and solution-extruded devices.

When pristine threads were annealed at 50 °C or more, we observe a characteristic maximum in the resistance at 40–46 °C for both types of threads (Figure 7a).

As one expects, the previous thermal history of the threads is retained; thus, when threads previously annealed at 60 °C are subsequently heated to 90 °C, the maximum near 45 °C is no longer apparent; instead, a new resistance maximum is observed (Figure 7b) before the resistance decreases at 65.5 °C ± 1.1 and 73.4 °C ± 2.2 °C, for the solution-extruded and -cast devices, respectively. We attribute these increases in resistance (Figure 7a) in part to volume expansion and reorganization, observed in other composites,[26,31] as crystalline regions of polyvinyl acetate and polyethylene become amorphous.[6,8]

Figure 8 shows the resistance of two pairs of pristine cast and extruded threads as they are heated to 129 °C and cooled back to 25 °C. Again, these samples show the characteristic

resistance cliff when heated, before the resistance decreases precipitously. There is an inflection (i.e., $\delta R/\delta T$ minimum) centered at 56–58 °C and 61–63 °C for the extruded and cast threads, respectivly.

When the samples are cooled back to 25 °C, the resistance of the threads increases with the inflection centered at 62 °C ± 1 °C for all four samples. The inflections coincide with the PEVA freezing point (64 and 61 °C Dupont Elvax 460 and 450, respectively).

Heating above 90 °C made the extruded samples too fragile and not usable after these treatments. The cast threads were also more brittle after >90 °C treatments, but were strong enough to still be attached to support pins for use as chemiresistors. Samples heated above 90 °C showed 5- to 10-fold improvement, versus pristine threads, as indicated by LOD values (Table 2) and benzene response profiles (Figure 9).

The post-anneal measurement noise (averaged of 10 sensors used in Table 2 calculations) in dry air and humid (50%) air from these tests was nearly identical, 7.0×10^{-6} Ω/Ω vs 7.3×10^{-6} Ω/ Ω, respectively. Some longer-term (minutes) variability can be attributed to the limits of humidity control of the test system, which can add to the observed error in the responses. The presence of humidity also diminishes the response, as the large amount of water vapor competes with benzene for binding sites in the polymer. Even though PEVA does not have a significant sensitivity to humidity, the acetate group in the polymer is capable of hydrogen bonding with water; thus, humidity in the carrier air may act to reduce the swelling of the polymer when benzene is added.

DSC

Four types of samples were submitted for DSC; a pristine PEVA18 “pellet”, PEVA18 dissolved in toluene cast without graphene, solution-cast nanocomposite before annealing, and cast nanocomposite after the 90 °C anneal (Figure 10).

No notable features were observed above 100 °C for any of the samples. During the heating, the PEVA samples without graphene show endothermic inflections or minima that occur in the range usually attributed to the melting temperatures of vinylacetate (49 °C) and polyethylene (77 °C). In comparison, Dadbin[4] shows pristine PEVA18 having a valley minimum at 84.7 °C, which is consistent with the PEVA pellet and cast film (81.2 and 80.2 °C, respectively). These endothermic phase transitions[26] during heating coincide with the observed maxima in the resistance measurements above, and the minima in the heat flow curves coincide with the observed change in TCR direction (80 °C).

The presence of graphene depresses the PEVA18 melting point, to 77.6 and 77.0 °C, for the unannealed and 90 °C annealed samples, respectively. In addition, the annealed sample shows more intense endothermic peaks in the low temperature range (<60 °C) compared to the unannealed nanocomposite. After the ≥80 °C heat-treatments, the threads were cooled at a maximum rate of 5 °C/min, slow enough to allow crystallization during cooling, which appears to affect the relative size of the endothermic peaks.

During cooling from 200 °C, the graphene-laden samples exhibit higher onset and peak freezing temperatures compared to the PEVA without graphene, which is due to the

graphene nucleating crystallization sites.[25,32] Without graphene, the freezing peaks are relatively sharp, but with graphene, the freezing peaks are broader, indicating a wider distribution of crystal sizes.[33] PEVA18 (room temperature) crystallinity is typically reported as only 25–26%.[6,9] Based on the earlier onset and peak crystallization temperature, we speculate that the annealed threads may have higher crystallinity than the unannealed threads. Higher crystallinity may explain the observed brittleness of the threads annealed at 90 °C and above.

Typically, the percolation threshold for chemiresistors is lower for a semicrystalline composite compared to an amorphous polymer-composite.[30] Further, positive and negative shifts in T_g and T_m have been reported for various composites, depending on processing, type of conductive filler, and cross-linking.[25,26,30,34] These effects are attributed to interfacial stresses between the polymer and the filler, and their relation to crystal nucleation and growth. From these results, it is still unclear whether the observed resistivity decrease, and reduced noise are directly related to total crystallinity, the size of the crystals, or simply improved dispersion of the graphene. For example, growth of larger crystals and the resulting reduction of the number of grain boundaries both can explain the observed lower resistivity and noise. Further, during the anneal, improved wetting of the graphene by the polymer may allow for better distribution prior to crystallization.[30]

SEM

Samples were investigated using scanning electron microscopy (SEM) to study the morphology of the polymer-composite. Both solution-cast and solution-extruded samples were studied as-fabricated and post 90 °C treatment. In Figure 11, the unannealed, solution-cast sample surface is smoother than the extruded sample, with regions of varied surface texture, ranging from smooth or amorphous to mottled with “bubbles” or rounded features (>1 μm to ≈50 nm). The cross section of the solution-cast sample appears relatively more uniform in texture.

In contrast, the solution-extruded surface morphology is more jagged, with regions of sharp features (few μm to tens of μm) in a background of more amorphous material. This is likely due to the shearing and stretching of the surface bubbles (air or solvent) that occurred when the sample was forced out of the steel syringe needle. It is unclear from this work if the sharp features are graphene agglomerates (7% by weight, 3% by volume) or PEVA18 crystals.

The result of the 90 °C anneal is a significantly rougher surface texture for both the cast and the extruded threads (Figure 12), and the two thread types are now less distinguishable under high magnification.

On a large scale, the surface morphology has become more consistent in appearance across the entire sample, with rugged terrain, and the polymer forming thin walls ($\ll 1$ μm) around voids or pores; the material surrounding the pores has the appearance of torn edges. One possible explanation for the appearance of these features is that they result from trapped solvent or water vapor escaping when the material is heated. The overall volume expansion

of the extruded thread is obvious when compared to the unannealed sample at the lowest magnification. Note that the extruded threads retained the cylindrical shape.

Both cast and extruded threads expanded after annealing (Table 1), increasing the void-space. The annealed samples have shorter response times. The faster responses may be attributed to the increased surface area and reduced bulk density (greater void space) allowing for faster vapor sorption and diffusion.

However, the baseline resistances (and volume resistivity, in dry air at 25 °C) and the noise in the resistance measurements of both types of annealed samples are significantly reduced (dropping from tens of kΩ to <500Ω), which is counterintuitive to the reduced bulk-density. We speculate that during the treatment above T_m, graphene redistributes, allowing significant agglomeration, prior to, or during, recrystallization when cooled. This improved distribution leads to reduced resistivity and noise. DSC results showed that graphene raises the onset of freezing, perhaps leading to increased crystallinity compared to undoped PEVA18. The role of crystallinity and the dispersion of graphene in the bulk require further study.

SUMMARY

Chemiresistive threads were fabricated using solution-casting and solution-extrusion of polymer–graphene composites. Electrical resistance of the threads thus fabricated increases substantially when exposed to benzene vapor, consistent with the concept of using the threads as chemical sensors to detect the presence and concentration of benzene in air. Both fabrication methods are compatible with low-cost thread fabrication techniques; further development would be required to optimize either method for high-volume production of threads that are physically robust and chemically sensitive enough for the intended application. More detailed electrical characterization could elucidate the relative influence of benzene's impact on the polymer or graphene-surface potential, as it relates to the observed resistance changes.

The limit of detection achieved from 15 min exposures of the threads to benzene vapor were used to compare various fabrication methods and thermal treatments. The sensitivity and speed of response were directly affected by physical characteristics of the threads and the thermal treatments they received during fabrication. Using 90 °C-annealed threads, LODs of 1.5 ± 0.1 ppm and 4 ± 3 ppm were achieved for benzene in dry and humid air, respectively, which is below the current U.S. OSHA short-term standard (5 ppm). This reflects roughly a 10× improvement over the unannealed threads.

DSC revealed that the presence of graphene raises the onset of freezing and lowers the melting point. Annealing followed by slow cooling appears to increase the crystallinity, which may help explain the observed reduction in resistivity, noise, and LOD. Crystal growth may be occluding graphene, creating more densely packed conduction pathways, that encounter fewer grain boundaries. The exact role of the graphene on the final distribution of crystals needs further study.

The annealing treatments, 90–129 °C, caused an increase in bulk volume, surface roughness, and a significant decrease in the measured electrical noise and baseline resistance. SEM showed surface roughening from the annealing; the higher surface area and development of significant void space is believed to be responsible for the observed faster responses and recovery. We speculate that the improved limits of detection observed after annealing are a result of several factors working in concert, including a significant change in the graphene dispersion and agglomeration, reducing physical strain in the threads,[31] which may lead to overall reduction in noise, the increased surface area allowing more area for vapor sorption, and the increased void-space improving bulk-diffusion.

The threads were compatible with the requirements of smart clothing-based chemical detectors, and with further optimization of the physical properties, more robust threads can be made. It is likely that the benzene sensitivity can be further improved by optimizing the graphene content of the nano-composite formulation. The sensors can also be made more sensitive by reducing the thread thickness, although this will make the threads more fragile. Microstructural changes caused by the thermal treatements appear to be a useful complement to improve sensitivity of polymer-based sensors along with modifications to polymer or graphene functionality. This thermal treatment may also be used with other, similar polymers to build diverse arrays, to detect other types of chemicals.

Acknowledgments

This work was partially supported by NIH CDC SBIR grant #R43OH010881, funded by the Centers for Disease Control and Prevention. Its contents are solely the responsibility of the authors and do not necessarily represent the official views of the Centers for Disease Control and Prevention or the Department of Health and Human Services. This work was performed in part at the San Diego Nanotechnology Infrastructure (SDNI) of UCSD, a member of the National Nanotechnology Coordinated Infra-structure (NNCI), which is supported by the National Science Foundation (Grant ECCS-1542148). The authors thank Professor Prabhakar Bandaru at the University of California, San Diego, for his valuable input on nanocomposite distribution and polymer conductivity.

References

1. Briglin SM, Freund MS, Tokumaru P, Lewis NS. Exploitation of Spatiotemporal Information and Geometric Optimization of Signal/noise Performance Using Arrays of Carbon Black-Polymer Composite Vapor Detectors. Sens Actuators, B. 2002; 82:54–74.
2. Hopkins AR, Lewis NS. Detection and Classification Characteristics of Arrays of Carbon Black/ organic Polymer Composite Chemiresistive Vapor Detectors for the Nerve Agent Simulants Dimethylmethylphosphonate and Diisopropylmethylphosponate. Anal Chem. 2001; 73:884–892. [PubMed: 11289432]
3. Kim YS, Ha SC, Yang Y, Kim YJ, Cho SM, Yang H, Kim YT. Portable Electronic Nose System Based on the Carbon Black–polymer Composite Sensor Array. Sens Actuators, B. 2005; 108:285–291.
4. Dadbin S, Frounchi M, Sabet M. Studies on the Properties and Structure of Electron-Beam Crosslinked Low-Density Polyethylene/ poly[ethylene-Co-(Vinyl Acetate)] Blends. Polym Int. 2005; 54:686–691.
5. Faker M, Razavi Aghjeh MK, Ghaffari M, Seyyedi SA. Rheology, Morphology and Mechanical Properties of Polyethylene/ ethylene Vinyl Acetate Copolymer (PE/EVA) Blends. Eur Polym J. 2008; 44:1834–1842.
6. Heuchel M, Al-Qaisi L, Kratz K, Nöchel U, Behl M, Lendlein A. Thermomechanical Characterization of a Series of Crosslinked Poly[Ethylene-Co-(Vinyl Acetate)] (PEVA) Copolymers. MRS Online Proc Libr. 2015; 1718:123–130.

7. Song WL, Veca LM, Kong CY, Ghose S, Connell JW, Wang P, Cao L, Lin Y, Meziani MJ, Qian H, et al. Polymeric Nanocomposites with Graphene Sheets - Materials and Device for Superior Thermal Transport Properties. Polymer. 2012; 53:3910–3916.
8. Pinkerova M, Polansky R. Influence of Cross-Linking on Properties of PEVA Used for Cable Sheaths. Ann DAAAM Proc Int DAAAM Symp. 2011; 22:975–976.
9. Hiss R, Hobeika S, Lynn C, Strobl G. Network Stretching, Slip Processes, and Fragmentation of Crystallites during Uniaxial Drawing of Polyethylene and Related Copolymers. A Comparative Study. Macromolecules. 1999; 32:4390–4403.
10. Themal Properties of Elvax Measured by Differential Scanning Calorimeter (DSC), Dupont Technical Data Sheet. http://www.dupont.com/products-and-services/plastics-polymers-resins/ethylene-copolymers/brands/elvax-ethylene-vinyl-acetate.html
11. http://www.sigmaaldrich.com/catalog/product/aldrich/437239?lang=en&region=US.
12. Freund MS, Lewis NS. A Chemically Diverse Conducting Polymer-Based “electronic Nose. Proc Natl Acad Sci U S A. 1995; 92:2652–2656. [PubMed: 11607521]
13. Patel SV, Jenkins MW, Hughes RC, Yelton WG, Ricco AJ. Differentiation of chemical components in a binary solvent vapor mixture using carbon/polymer composite-based chemiresistors. Anal Chem. 2000; 72:1532. [PubMed: 10763250]
14. Hughes RC, Yelton WG, Pfeifer KB, Patel SV. Characteristics and Mechanisms in Ion-Conducting Polymer Films as Chemical Sensors Polyethyleneoxide. J Electrochem Soc. 2001; 148:H37.
15. Eastman MP, Hughes RC, Yelton G, Ricco AJ, Patel SV, Jenkins MW. Application of the Solubility Parameter Concept to the Design of Chemiresistor Arrays. J Electrochem Soc. 1999; 146:3907–3913.
16. Kim SK, Burris DR, Chang H, Bryant-Genevier J, Zellers ET. Microfabricated Gas Chromatograph for on-Site Determination of Trichloroethylene in Indoor Air Arising from Vapor Intrusion. 1. Field Evaluation. Environ Sci Technol. 2012; 46:6065–6072. [PubMed: 22616709]
17. Sharma S, Hussain S, Singh S, Islam SS. MWCNT-Conducting Polymer Composite Based Ammonia Gas Sensors: A New Approach for Complete Recovery Process. Sens Actuators, B. 2014; 194:213–219.
18. Wang T, Huang D, Yang Z, Xu S, He G, Li X, Hu N, Yin G, He D, Zhang L. A Review on Graphene-based Gas/Vapor Sensors with Unique Properties and Potential Applications. Nano-Micro Lett. 2016; 8:95–119.
19. Benz M, Patel SV. Freestanding Chemiresistive Polymer Composite Ribbons as High-Flux Sensors. J Appl Polym Sci. 2012; 125(5):3986–3995.
20. Hansen, CM. A User’s Handbook. CRC Press; Boca Raton, FL: 2000. Hansen Solubility Parameters; p. 192Parameters given in the text are approximated from values of Elvax 150 and Elvax 250, which have higher vinyl acetate content than the PEVA used in this work
21. Barton, AFM. CRC Handbook of Solubility Parameters and Other Cohesion Parameters. 2. CRC Press; Boca Raton, FL: 1983. p. 414
22. Hobson ST, Cemalovic S, Patel SV. Preconcentration and Detection of Chlorinated Organic Compounds and Benzene. Analyst. 2012; 137:1284–1289. [PubMed: 22266477]
23. Patel SV, Hobson ST, Cemalovic S, Mlsna TE. Detection of Methyl Salicylate Using Polymer-Filled Chemicapacitors. Talanta. 2008; 76:872–877. [PubMed: 18656672]
24. Mlsna TE, Cemalovic S, Warburton M, Hobson ST, Mlsna DA, Patel SV. Chemicapacitive Microsensors for Chemical Warfare Agent and Toxic Industrial Chemical Detection. Sens Actuators, B. 2006; 116:192–201.
25. Li Q, Xue QZ, Gao XL, Zheng QB. Temperature Dependence of the Electrical Properties of the Carbon Nanotube/ polymer Composites. eXPRESS Polym Lett. 2009; 3:769–777.
26. Chung DDL. Thermal analysis of carbon fiber polymer-matrix composites by electrical resistance measurement. Thermochim Acta. 2000; 364:121–132.
27. Currie LA. Nomenclature in Evaluation of Analytical Methods Including Detection and Quantification Capabilities (IUPAC Recommendations 1995). Pure Appl Chem. 1995; 67:1699–1723.
28. Currie LA. Detection and quantification limits: origins and historical overview. Anal Chim Acta. 1999; 391:127–134.

29. Simplified relation for the limit of detection based on the IUPAC standard; assumes constant standard deviation, and requires = 95% confidence of positive detection.
30. Al-Saleh MH, Sundararaj U. A review of vapor grown carbon nanofiber/polymer conductive composites. Carbon. 2009; 47(1):2–22.
31. Mei Z, Chung DDL. Thermal History of Carbon- Fiber Polymer-Matrix Composite, Evaluated by Electrical Resistance Measurement. Thermochim Acta. 2001; 369:87–93.
32. Huang CL, Lou CW, Liu CF, Huang CH, Song XM, Lin JH. Polypropylene/Graphene and Polypropylene/Carbon Fiber Conductive Composites: Mechanical, Crystallization and Electromagnetic Properties. Appl Sci. 2015; 5:1196–1210.
33. Stark W, Jaunich M. Investigation of Ethylene/Vinyl Acetate Copolymer (EVA) by thermal analysis DSC and DMA. Polym Test. 2011; 30:236–242.
34. Robertson CG, Lin CJ, Rackaitis M, Roland CM. Influence of Particle Size and Polymer-Filler Coupling on Viscoelastic Glass Transition of Particle-Reinforced Polymers. Macromolecules. 2008; 41:2727–2731.

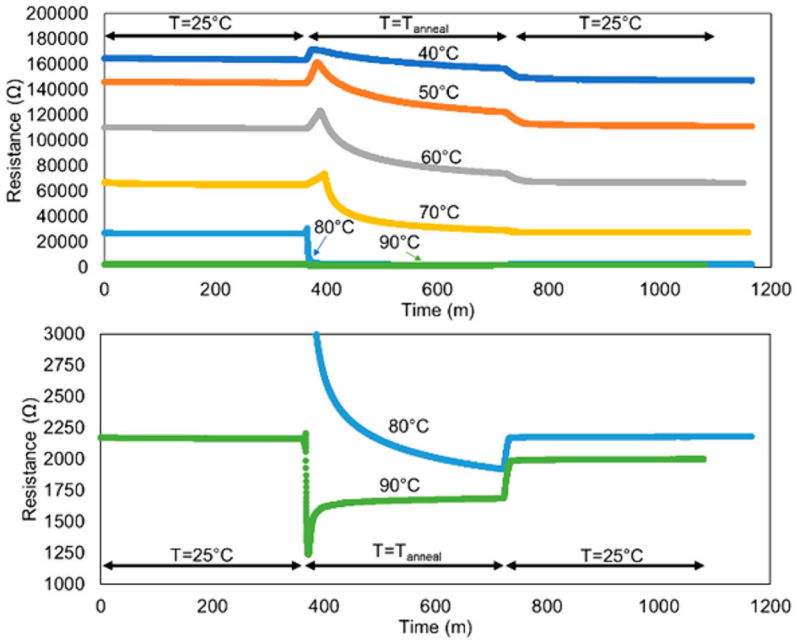

Figure 1.

Resistance traces from extruded 22-gauge thread (upper) during successive anneals and close-up (lower) of the 80 and 90 °C treatments. Anneals were conducted in air 6 h at 25 °C, 6 h at T_{anneal}, followed by 6 h at 25 °C. Heating rate was 7.5 °C/min for anneals to 70 and 8.4 °C/min for the 80 and 90 °C anneals. Cooling rates were 0.7 °C/min for anneals from 70 °C and below, and 5 °C/min for the 80 and 90 °C anneals.

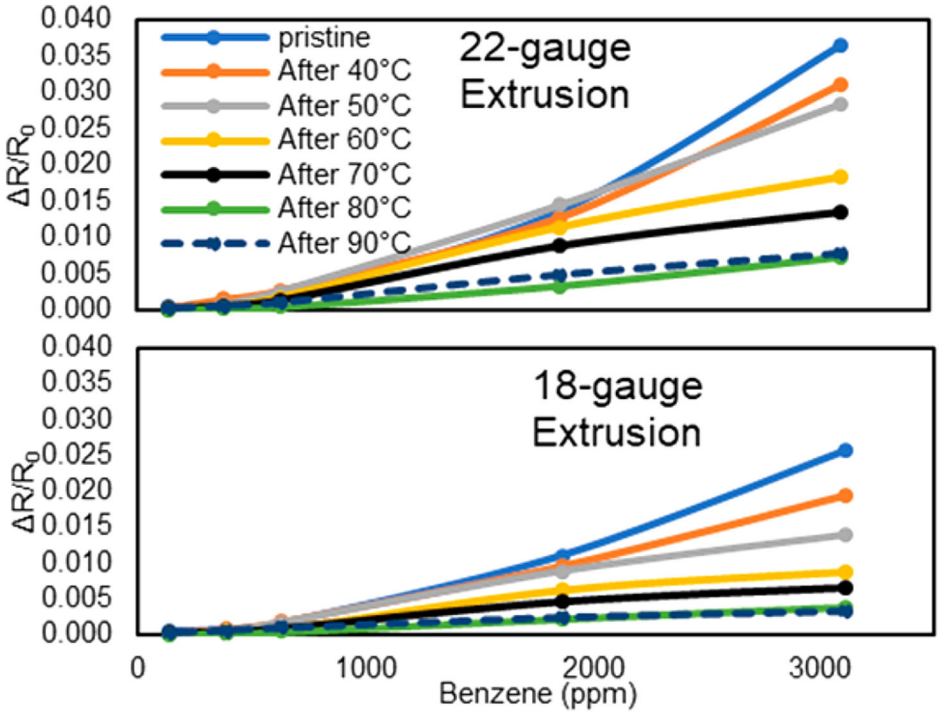

Figure 2.
Response profiles for extruded threads exposed to benzene (15 min exposures) in dry air at 25 °C.

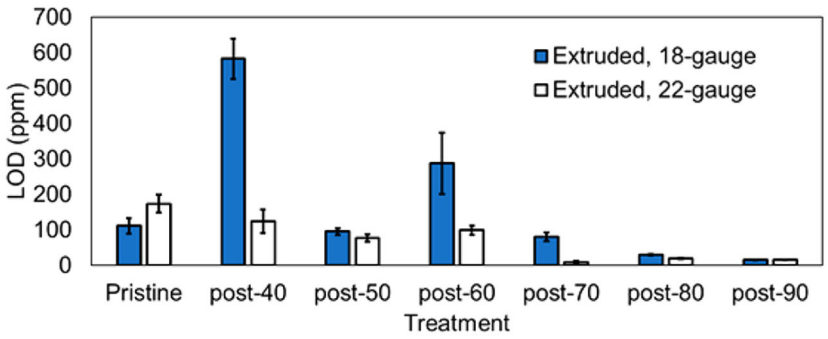

Figure 3.

Average limits of detection for benzene (628 ppm V exposure) in dry air from extruded threads. Error bars denote ± 1 standard deviation.

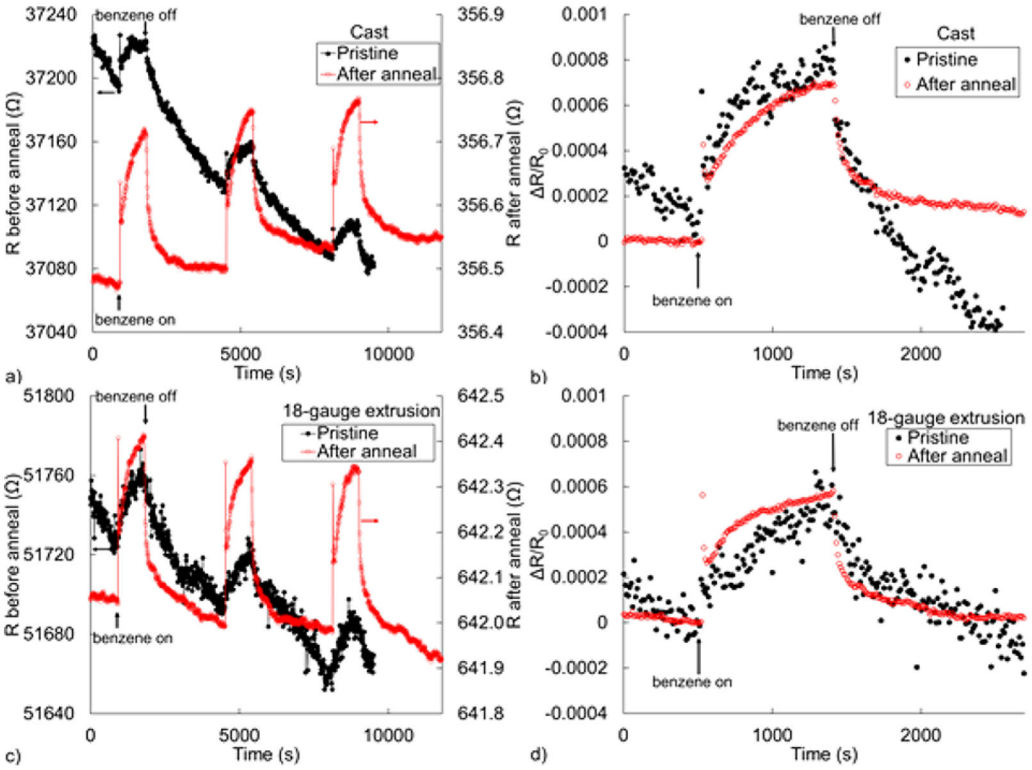

Figure 4.

Responses from three benzene exposures (124 ppm V) in dry air for (a,b) solution-cast and (c,d) solution-extruded sensors before (black) and after (red) the 90 °C anneal. Close-up views of a single exposure (b) and (d) are normalized to show the relative noise and response speed.

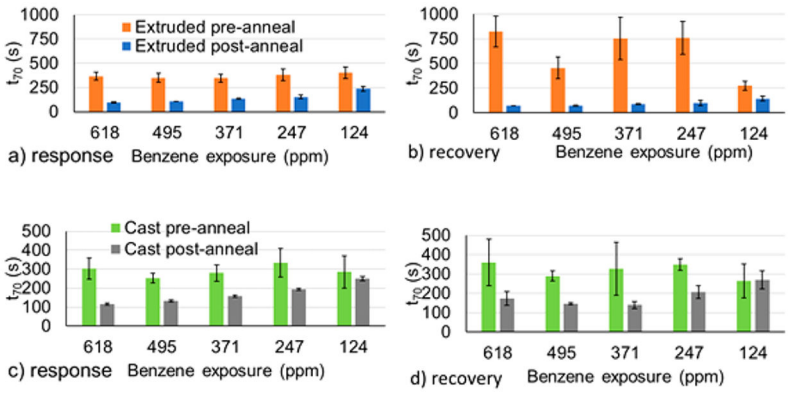

Figure 5.

Average time to achieve 70% of the resistance change (t_{70}) during (a,c) response to and (b,d) recovery from benzene exposures (n = 3) in dry air at 25 °C for the extruded (top row) and response and cast (bottom row) samples. Error bars = ±1 SD.

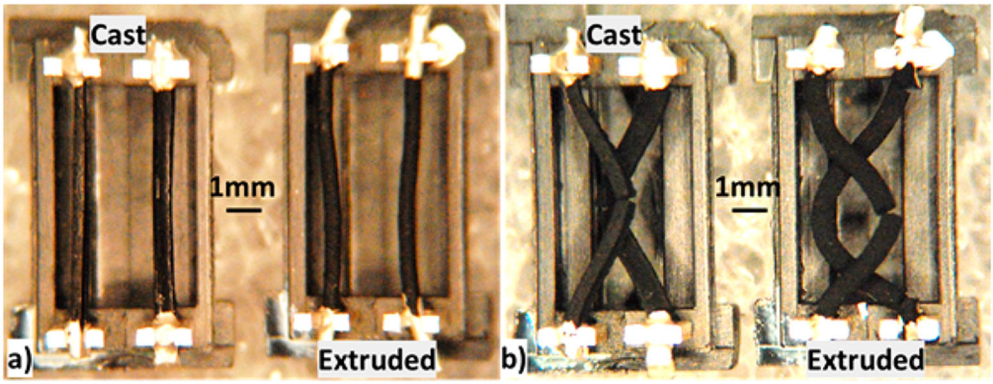

Figure 6.

(a) Cast and solution-extruded sensors prior to annealing, and (b) the same devices after 129 °C anneal, showing volume expansion and structural breaks.

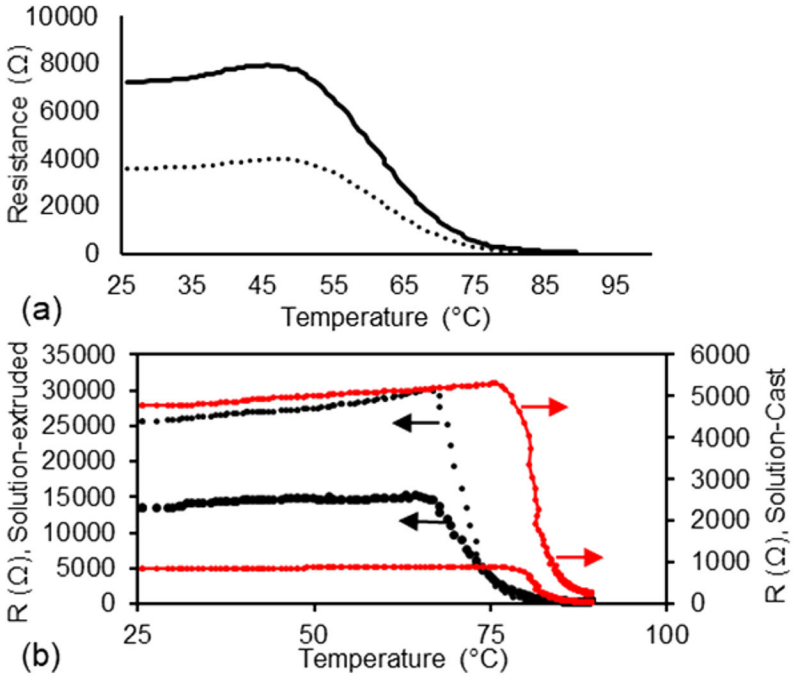

Figure 7.

(a) Resistance of two pristine solution-cast samples first heating to 90 °C. (b) Previously 60 °C-annealed solution-extruded (black) and cast (red) samples (two each), first heating to 90 °C. Heating rate was 7.5 °C/min.

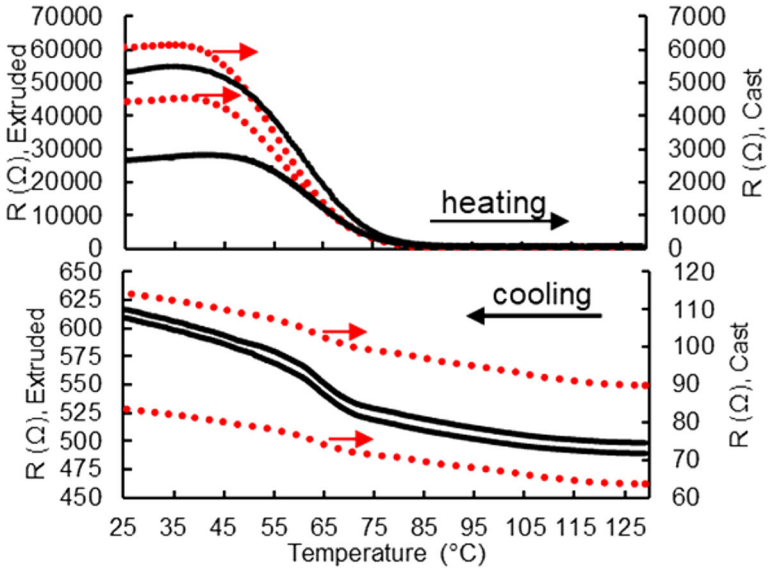

Figure 8.

(upper) Resistance traces for pristine solution-cast (dashed lines, right axis) and solution-extruded (solid lines, left axis) samples during heating from 25 to 129 °C (0.2 °C/min), and (lower) during cooling (4 °C/min) to 25 °C..

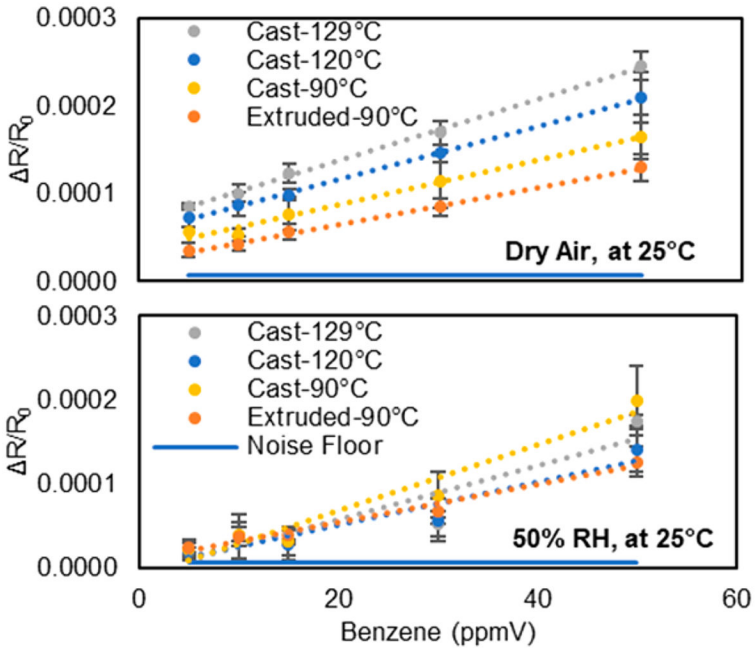

Figure 9.

Benzene response profiles, in dry and humid air, from cast and solution-extruded threads after anneals at 90, 120, and 129 °C. The standard error of the baseline is indicated by the horizontal solid line in both plots.

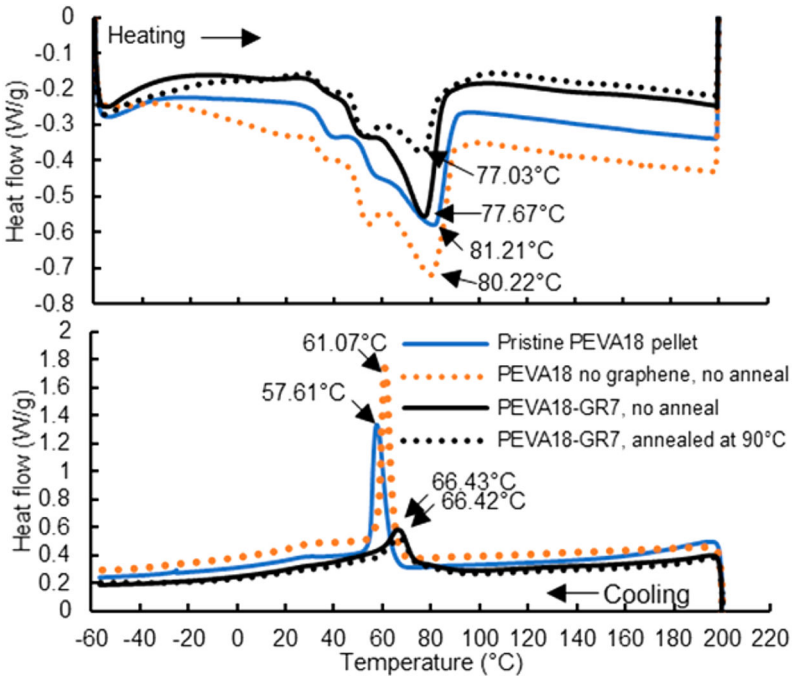

Figure 10.

DSC heat flow (endothermic downward) from samples of pristine PEVA18 without processing, PEVA18 cast from solution without graphene, 90 °C annealed solution-cast. Samples were heated (upper) to 200 °C then cooled (lower) back to −60 °C.

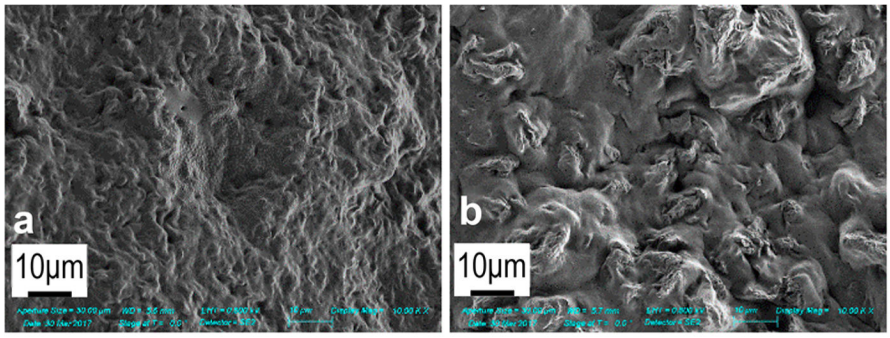

Figure 11.
SEM images (10,000×) of a (a) solution-cast and (b) solution-extruded sample surfaces before thermal treatment.

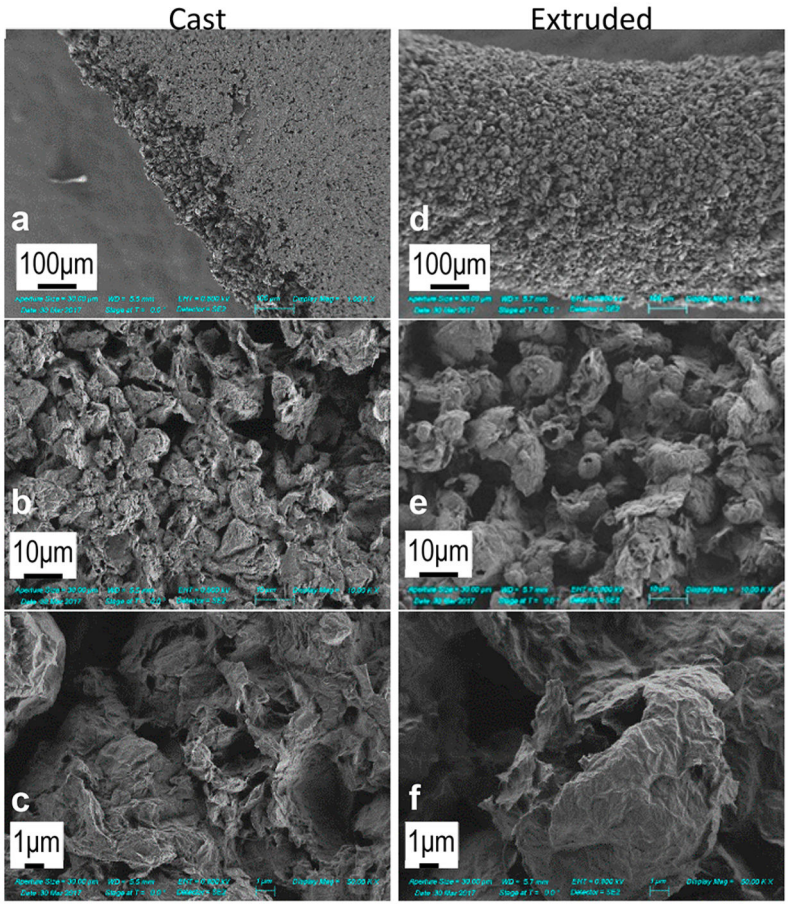

Figure 12.
SEM images of (a–c) solution-cast and (d–f) solution-extruded sample surfaces after 90 °C anneal.

Table 1

Average Percentage Volume Expansion of (90 °C) Annealed Samples (Two of Each Type)[a]

measured dimension	cast	extruded
Length	4.0%	18.3%
Thickness	5.4%	
Width or Diameter	10.8%	14.8%
Volume expansion	27%	69%

[a]When heated to 90 °C unconstrained, the solution-extruded threads bend, as the stress is apparently not consistent on all sides. The solution-cast segments, which are thicker, stay straighter when annealed unconstrained.

Table 2

Limits of Detection for Benzene from Figure 9 Data in Dry Air and 50% Humidity at 25 ℃

	limit of detection (ppm)	
type, anneal temperature	**dry air**	**50% humidity**
Extruded, Pristine	48 ± 9	Not tested
Extruded, 90 °C	2.4 ± 0.6	4 ± 3
Cast, Pristine	21 ± 9	Not tested
Cast, 90 °C	2.5 ± 2.1	9 ± 6
Cast, 120 °C	2.2 ± 0.4	8 ± 4
Cast, 129 °C	1.5 ± 0.1	8 ± 1